Synthesis of Well-Defined 7-Arm and 21-Arm Poly(*N*-isopropylacrylamide) Star Polymers with *β*-Cyclodextrin Cores via Click Chemistry and Their Thermal Phase Transition Behavior in Aqueous Solution

JIAN XU, SHIYONG LIU

Key Laboratory of Soft Matter Chemistry, Department of Polymer Science and Engineering, Hefei National Laboratory for Physical Sciences at the Microscale, University of Science and Technology of China, Hefei, Anhui 230026, China

Received 25 August 2008; accepted 13 October 2008
DOI: 10.1002/pola.23157
Published online in Wiley InterScience (www.interscience.wiley.com).

ABSTRACT: The syntheses of well-defined 7-arm and 21-arm poly(*N*-isopropylacrylamide) (PNIPAM) star polymers possessing *β*-cyclodextrin (*β*-CD) cores were achieved via the combination of atom transfer radical polymerization (ATRP) and click reactions. Heptakis(6-deoxy-6-azido)-*β*-cyclodextrin and heptakis[2,3,6-tri-*O*-(2-azidopropionyl)]-*β*-cyclodextrin, *β*-CD-$(N_3)_7$ and *β*-CD-$(N_3)_{21}$, precursors were prepared and thoroughly characterized by nuclear magnetic resonance and matrix-assisted laser desorption/ionization time-of-flight mass spectrometry. A series of alkynyl terminally functionalized PNIPAM (alkyne-PNIPAM) linear precursors with varying degrees of polymerization (DP) were synthesized via atom transfer radical polymerization (ATRP) of *N*-isopropylacrylamide using propargyl 2-chloropropionate as the initiator. The subsequent click reactions of alkyne-PNIPAM with *β*-CD-$(N_3)_7$ and *β*-CD-$(N_3)_{21}$ led to the facile preparation of well-defined 7-arm and 21-arm star polymers, namely *β*-CD-$(PNIPAM)_7$ and *β*-CD-$(PNIPAM)_{21}$. The thermal phase transition behavior of 7-arm and 21-arm star polymers with varying molecular weights were examined by temperature-dependent turbidity and micro-differential scanning calorimetry, and the results were compared to those of linear PNIPAM precursors. The anchoring of PNIPAM chain terminal to *β*-CD cores and high local chain density for star polymers contributed to their considerably lower critical phase separation temperatures (T_c) and enthalpy changes during phase transition as compared with that of linear precursors. © 2008 Wiley Periodicals, Inc. J Polym Sci Part A: Polym Chem 47: 404–419, 2009
Keywords: atom transfer radical polymerization (ATRP); star polymers; stimuli-sensitive polymers

INTRODUCTION

Because of their branched architecture and unique physicochemical properties compared with those of linear counterparts; star polymers have received ever-increasing interests over the past few decades.[1–3] The synthesis of star polymers can be generally categorized into two strategies, namely the "arm-first" and "core-first" approaches. The first one relies on the preparation of terminally functionalized linear chains followed by covalently coupling to multifunctional cores; in

Correspondence to: S. Liu (E-mail: sliu@ustc.edu.cn)
Journal of Polymer Science: Part A: Polymer Chemistry, Vol. 47, 404–419 (2009)

the core-first approach, a multifunctional initiator is employed to grow arms via various controlled polymerization techniques.[1,2] It should be noted that recent advances in controlled radical polymerizations have rendered possible the facile architectural control of star polymers and the choice from a variety of monomers.[4–11]

Being highly biocompatible and readily available, β-cyclodextrin (β-CD) is one of the excellent candidates as core materials for the synthesis of star polymers.[12] β-CD is a cyclic oligosaccharide consisting of seven glucose units linked by α-1,4-glucosidic bonds with fixed numbers of primary (7) and secondary (14) hydroxyl groups, which can be further utilized for selective modification and surface grafting. Using the core-first approach, a variety of star polymers have been synthesized via nitroxide-mediated polymerization (NMP),[13] atom transfer radical polymerization (ATRP),[14–16] and reversible addition-fragmentation chain transfer (RAFT)[17,18] polymerization using β-CD-based multifunctional initiators.[19–27] Haddleton and coworkers[23] first reported the synthesis of 21-arm poly(methyl methacrylate) (PMMA) or polystyrene (PS) star polymers based on fully functionalized β-CD. Stenzel et al.[25,26] reported the synthesis of 7-arm PS star polymer by RAFT technique using β-CD bearing heptafunctional trithiocarbonate moieties as the RAFT agent. Kakuchi and coworkers[19,22] described the synthesis of 7-arm PS by NMP technique using nitroxide-functionalized β-CD as initiator. However, grafting multi-arms starting from functionalized β-CD via controlled radical polymerization techniques can lead to high local concentrations of free radicals, especially at the early stages of polymerization. Thus, side reactions such as star-star coupling and intramolecular radical termination might occur, leading to star polymers with less well-defined architectures.

Recently, Sharpless et al.[28,29] popularized the 1,3-dipolar cycloaddition of azides and terminal alkynes in the presence of copper(I) catalytic species. Because of the fidelity, high efficiency, and operational simplicity, this novel type of cycloaddition reaction was classified as "click" chemistry. Matyjaszewski and Gao[30] reported the synthesis of 3-arm and 4-arm star PS by employing a combination of ATRP and click chemistry. Schubert and coworkers[31] reported the synthesis of 7-arm star poly(ε-caprolactone) (PCL) via click reaction using alkynyl-functionalized linear PCL precursor, starting from heptakis(6-deoxy-6-azido)-β-cyclodextrin. Thus, click reaction can be facilely employed for the preparation of well-defined star polymers with controlled number of arms.[32–43]

It should be noted that almost all the aforementioned star polymers based on CD are water-insoluble.[19–27,31] Our recent research interests focused on stimuli-responsive water-soluble polymers. Poly(*N*-isopropylacrylamide) (PNIPAM) has been the most extensively studied thermoresponsive polymer, which exhibits a lower critical solution temperature (LCST) phase behavior in aqueous solution.[44] It has also been generally accepted that the spatial arrangement of PNIPAM chains can dramatically affect the phase transition behavior.[45] When PNIPAM chains are tethered to curved surfaces such as latex particles,[46–48] gold nanoparticles,[49,50] and microgels,[51] the inner part of PNIPAM segments close to the spherical core will be more densely packed than the outer part of PNIPAM segments.[52] Napper and coworkers[46–48] observed two thermal phase transitions for PNIPAM chains adsorbed at the surface of latex particles. The first transition occurred above the θ-temperature of PNIPAM (30 °C), which is similar to that of free PNIPAM chains in aqueous solution. The second transition was observed at lower temperatures in the broad range 15–30 °C. This phenomenon was explained by invoking the n-cluster concept of de Gennes.[53,54] In this theory, the attractive n-body ($n > 2$) interactions can lead to n-clusters, which can induce the collapse of polymer brush. For polymer brush grafted at the surface of spherical core, the densely grafted inner layer has larger possibility to exhibit n-clustering induced collapse, as compared to the outer part of the brush. Napper and coworkers[46–48] also found that the n-cluster contribution increased significantly with decreasing molecular weights (MW) of surface-adsorbed PNIPAM brushes.

For PNIPAM brush tethered to gold nanoparticles, Tenhu and coworkers[49,50] also reported two phase transitions as revealed by microcalorimetry. They ascribed the phase transition at ~32 °C to that of the inner part of PNIPAM segments, and the phase transition at ~40 °C to that of outer part of PNIPAM segments. Whittaker and coworkers[55] recently synthesized 4-arm PNIPAM star polymers with varying MW employing a tetrafunctional RAFT agent, and observed n-cluster induced collapse for star polymers below LCST. However, they concluded that n-cluster contribution increased with increasing MW for star polymers, which is contrary to the that described by Napper and coworkers.[46–48]

In our previous report,[7] PNIPAM star polymers were prepared via reversible addition-fragmentation chain transfer (RAFT) polymerization of *N*-isopropylacrylamide (NIPAM) using hyperbranched polyester (Boltorn H40)-based macro-RAFT agent. It existed as unimolecular micelles with hydrophobic H40 as the core and densely grafted PNIPAM brush as the shell. The average grafting density of corona PNIPAM chains at the core surface was estimated to be 0.46 nm^2 per chain. We established that PNIPAM brush densely grafted at the surface of hydrophobic dendritic core exhibits double thermal phase transition behavior. The inner part of PNIPAM brush collapses at lower temperatures (<30 °C) due to *n*-cluster induced collapse resulting from the high local chain density; above 30 °C, the outer part of PNIPAM brush starts to collapse. However, the structure (number of arms, grafted chain lengths) of PNIPAM star polymer in this example was less well-defined as a core-first approach was employed on the basis of hyperbranched polyester (H40) with relatively broad polydispersity and nonuniform surface functional groups[7,8]; moreover, the chain-length effect of grafted PNIPAM arms on the thermal phase transition behavior has remained to be explored. Li and coworkers[56] recently present a novel β-CD core PNIPAM star polymer, β-CD-$(PNIPAM)_4$. That work demonstrated a self-assembling system comprising a star-shaped PNIPAM block and a hydrophilic PEG block, but required an elaborate synthesis of β-CD precursors.

In this report, we describe the thermal phase transition behavior of well-defined 7-arm and 21-arm PNIPAM star polymers, β-CD-$(PNIPAM)_7$ and β-CD-$(PNIPAM)_{21}$, which were prepared via click reactions between alkynyl terminally functionalized PNIPAM (alkyne-PNIPAM) with heptakis(6-deoxy-6-azido)-β-cyclodextrin and heptakis[2,3,6-tri-*O*-(2-azidopropionyl)]-β-cyclodextrin, β-CD-$(N_3)_7$, and β-CD-$(N_3)_{21}$, respectively. To the best of our knowledge, the preparation of 7-arm and 21-arm PNIPAM star polymers possessing β-CD cores has not been reported yet. Moreover, the thermal phase transition behavior in aqueous solutions of β-CD-$(PNIPAM)_7$ and β-CD-$(PNIPAM)_{21}$ star polymers with varying PNIPAM arm lengths were examined by temperature-dependent turbidity and micro-differential scanning calorimetry (micro-DSC), and the results were compared with those of linear PNIPAM precursor. The MW-dependence of the phase transition behavior of PNIPAM star polymers was elucidated.

EXPERIMENTAL

Materials

N-isopropylacrylamide (97%, Tokyo Kasei Kagyo) was recrystallized twice from benzene/hexane (65 : 35 v/v) prior to use. β-Cyclodextrin (β-CD, Sinopharm Chemical Reagent) was recrystallized twice from water, and dried under reduced pressure at 100 °C over P_2O_5 for 2 days. Copper(I) chloride (CuCl, 99%), copper(I) bromide (CuBr, 99%), 2,2-dipyridyl (bpy, 99%), propargyl alcohol (99%), and 2-bromopropionic bromide (97%) were purchased from Aldrich and used as received. 2-Chloropropionic acid (98%) was purchased from ABCR. Sodium azide (NaN_3, 99%) was purchased from Alfa Aesar. Merrifield Resin was purchased from GL Biochem (Shanghai) and used without further purification. Tris(2-aminoethyl)amine (TREN) (96%) was purchased from Acros and tris(2-(dimethylamino)ethyl)amine (Me_6TREN) was synthesized from TREN according to literature procedures.[57] *N,N*-dicyclohexyl-carbodimide (DCC), 4-dimethylaminopyridine (DMAP), 2-propanol, *N,N*-dimethylformamide (DMF), *N*-methyl-2-pyrrolidone (NMP), and all other chemicals were purchased from Sinopharm Chemical Reagent and used as received.

Synthesis

General procedures employed for the preparation of 7-arm and 21-arm star PNIPAM star polymers were shown in Scheme 1.

Synthesis of Heptakis(6-deoxy-6-azido)-β-cyclodextrin (β-CD-$(N_3)_7$)

The target compound was prepared according to procedures reported by Ashton et al.[58] Ph_3P (18.36 g, 70 mmol) was dissolved in dry DMF (100 mL) under stirring. I_2 (17.77 g, 70 mmol) was then carefully added over a period of 10 min, the solution temperature increased to ~70 °C after the addition was complete. Dry β-CD (5.68 g, 5 mmol) was then added to the dark brown solution. The mixed solution was stirred under N_2 atmosphere for 24 h at 70 °C. The solution was partially concentrated under reduced pressure (removal of ~60 mL DMF). Sodium methoxide (3.0 M in methanol, 30 mL) was then added under cooling with ice-water bath. The reaction mixture was poured into methanol (500 mL), the precipitates was washed with excess methanol and then dried in a vacuum oven for 2 h. After re-dissolving

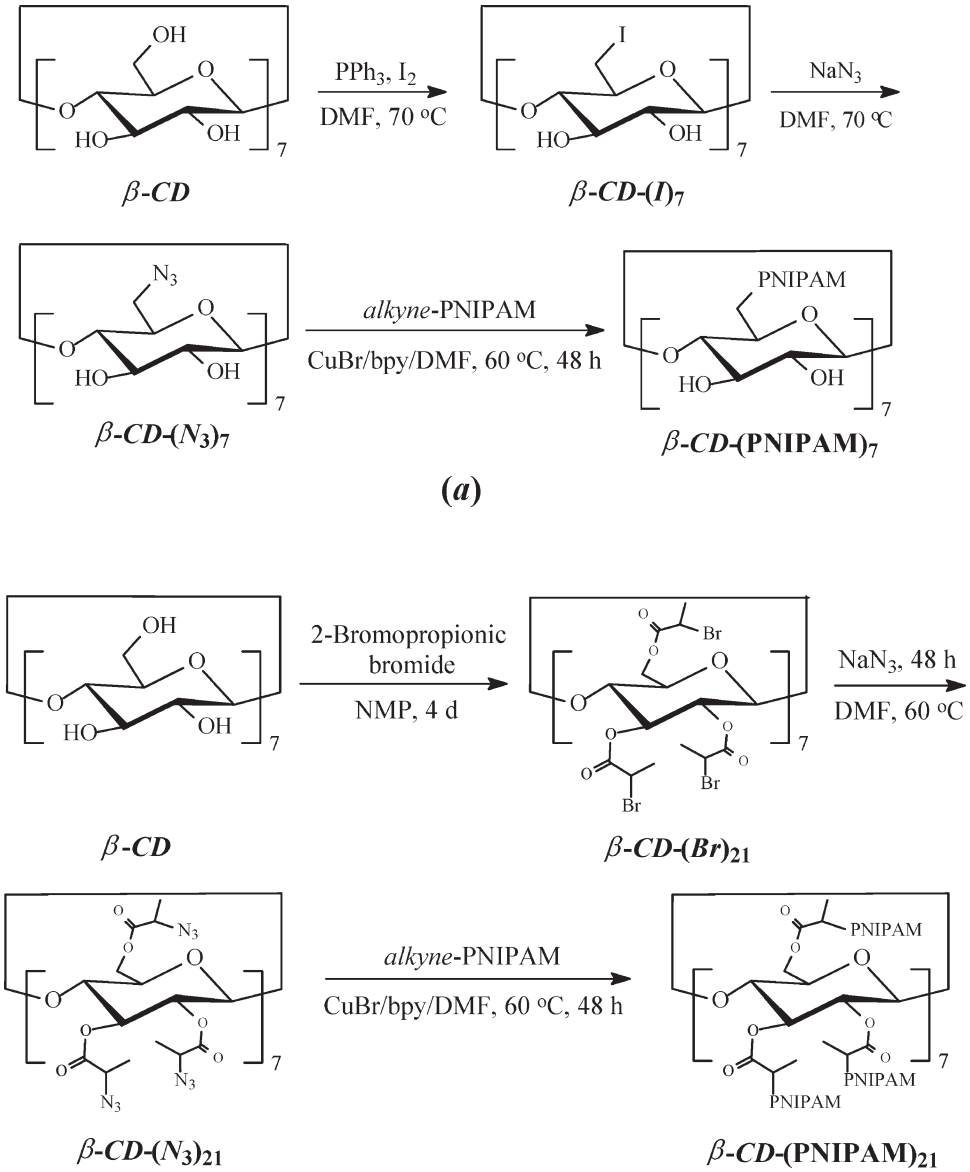

Scheme 1. Synthetic routes for the preparation of well-defined (a) 7-arm PNIPAM star polymers, β-CD-(PNIPAM)$_7$, and (b) 21-arm PNIPAM star polymers, β-CD-(PNIPAM)$_{21}$, via "click" reactions of alkyne-PNIPAM with β-CD-(N$_3$)$_7$ and β-CD-(N$_3$)$_{21}$, respectively.

in DMF, the above precipitation-drying cycle was repeated for five times. Heptakis(6-deoxy-6-iodo)-β-cyclodextrin was obtained as white solids after drying under vacuum at room temperature for 1 day.

Heptakis(6-deoxy-6-iodo)-β-cyclodextrin (4.62 g, 2.6 mmol) was dissolved in DMF (50 mL), and NaN_3 (2.02 g, 31 mmol) was added. The resulting suspension was stirred at 70 °C under an atmosphere of N_2 for 36 h. The suspension was then concentrated under reduced pressure before addition of an excess of water. A fine white powder (2.96 g, 87% yield) was obtained after filtration, washing with water, and drying in a vacuum oven. $M_{n,GPC} = 2100$, $M_w/M_n = 1.02$.

^{1}H-NMR in DMSO-d_6 (δ, ppm): 3.10–3.93 (42H, *H*-2, *H*-3, *H*-4, *H*-5, *H*-6), 4.87 (7H, *H*-1), 5.73 (7H, O*H*), 5.89 (7H, O*H*). ^{13}C-NMR in DMSO-d_6 (δ, ppm): 51.5 (*C*-6), 70.5 (*C*-5), 72.1 (*C*-2), 72.7 (*C*-3), 83.3 (*C*-4), 102.2 (*C*-1). MALDI-TOF MS m/z:

calcd for $C_{42}H_{64}O_{28}N_{21}$ ($M + H^+$), 1310.4; found, 1310.1.

Synthesis of Heptakis[2,3,6-tri-O-(2-bromopropionyl)]-β-cyclodextrin (β-CD-(Br)$_{21}$)[59]

A solution of 2-bromopropionic bromide (27.63 g, 128 mmol) in dry NMP (20 mL) was added dropwise into a solution of dry β-CD (2.27 g, 2 mmol) in dry NMP (30 mL) in an ice-water bath. After stirring at ambient temperature for 3 days and then under reduced pressure for 1 day, the brownish solution was diluted with methylene chloride (100 mL). The solution was successively washed with 1 N HCl, saturated aq. $NaHCO_3$ solution, 1 N aq. NaCl, and finally with water. The organic phase was dried over anhydrous Na_2SO_4 and concentrated using a rotary evaporator after filtration. The yellow-brownish residues were further purified by silica gel column chromatography using THF as eluent, yielding a colorless powder (1.11 g; 14% yield). $M_{n,GPC} = 4000$, $M_w/M_n = 1.02$.

^{1}H-NMR in $CDCl_3$ (δ, ppm): 1.86 (63 H, CH_3), 3.70–5.55 (70 H, sugar protons and BrCHCH$_3$ at ~4.47) ^{13}C-NMR in $CDCl_3$ (δ, ppm): 21.5 (*C*H$_3$), 39.9 (*C*HBr), 63.9 (*C*-6), 70.2–74.8 (*C*-1, *C*-4, *C*-5), 96.3 (*C*-2, *C*-3), 169.1 (*C* = O); MALDI-TOF MS m/z: calcd for $C_{105}H_{134}O_{56}Br_{21}$ ($M + H^+$), 3948.0; found, 3947.5.

Synthesis of Heptakis[2,3,6-tri-O-(2-azidopropionyl)]-β-cyclodextrin (β-CD-(N$_3$)$_{21}$)

β-CD-(Br)$_{21}$ was dissolved in DMF, NaN_3 (five times excess relative to bromine) was added, and the resulting solution was allowed to stir for 48 h at 60 °C. After precipitation from DMF into water, the residues was dissolved in THF, and passed through a neutral alumina column to remove residual salts. The obtained β-CD-(N$_3$)$_{21}$ was dried to constant weight under vacuum at room temperature. $M_{n,GPC} = 3200$, $M_w/M_n = 1.03$.

^{1}H-NMR in $CDCl_3$ (δ, ppm): 1.48 (63H, CH_3), 3.5–5.4 (70 H, sugar protons and N$_3$CHCH$_3$ at ~4.06). ^{13}C-NMR in $CDCl_3$ (δ, ppm): 16.5 (*C*H$_3$), 57.4 (*C*HN$_3$), 63.9 (*C*-6), 70.2–74.8 (*C*-1, *C*-4, *C*-5), 96.3 (*C*-2, *C*-3), 169.1 (*C* = O). MALDI-TOF MS m/z: calcd for $C_{105}H_{134}O_{56}N_{63}$ ($M + H^+$), 3173.0; found, 3172.8.

Synthesis of Azido-Functionalized Merrifield Resin

To a suspension of Merrifield resin (1% divinylbenzene, 200–400 mesh, ~0.8 mmol Cl/g; 2.0 g) and DMSO (20 mL) in a scintillation vessel, NaN_3 (520 mg, 8.0 mmol) was added. The reaction mixture was stirred at 60 °C for 3 days under N_2 atmosphere. After cooling to room temperature, the suspension was filtrated and the resin was thoroughly washed with water, mathanol and methylene chloride. After drying in a vacuum oven, azido-functionalized Merrifield resin was obtained.

Preparation of Propargyl 2-Chloropropionate

The ATRP initiator, propargyl 2-chloropropionate (PCP), was prepared by the esterification reaction of propargyl alcohol with 2-chloropropionic acid in the presence of DCC and DMAP. A typical procedure was as follows. A 250-mL round-bottom flask was charged with 2-chloropropionic acid (10.85 g, 0.10 mol), DCC (22.70 g, 0.11 mol), and methylene chloride (120 mL). The reaction mixture was cooled to 0 °C in an ice-water bath, and a mixture of propargyl alcohol (5.61 g, 0.10 mol), DMAP (0.5 g), and methylene chloride (30 mL) was added dropwise over a period of 1 h under magnetic stirring. After the addition was completed, the reaction mixture was stirred at 0 °C for 1 h and then at room temperature for 12 h. After removing insoluble *N,N*-dicyclohexylurea by suction filtration, the filtrate was concentrated and further purified by silica gel column chromatography using methylene chloride as the eluent. After removing the solvent by rotary evaporator, the obtained residues were distilled under reduced pressure. A colorless liquid was obtained with a yield of ~84%.

^{1}H-NMR ($CDCl_3$, δ, ppm): 4.76 (2H, —CH_2O—), 4.43 (1H, —CHCl—), 2.51 (1H, —C≡CH), and 1.70 (3H, —CH_3).

Synthesis of Alkyne-PNIPAM

A typical procedure employed for the preparation of alkyne-PNIPAM with a target degree of polymerization (DP) of 20 was as follows.[57] The solution mixture containing NIPAM (9.05 g, 80 mmol), Me_6TREN (922 mg, 4 mmol), and 2-propanol (18.10 g) was deoxygenated by bubbling with nitrogen for at least 30 min. CuCl (316 mg, 3.2 mmol) was introduced under the protection of N_2 flow. The reaction mixture was stirred for ~10 min to allow the formation of CuCl/Me_6TREN complex. PCP (586 mg, 4 mmol) was then added via a syringe to start the polymerization. The reaction was carried out at 25 °C and allowed to stir under N_2 atmosphere for 5 h, followed by

quenching into liquid nitrogen to stop the polymerization. The reaction mixture was precipitated into an excess of *n*-hexane. The sediments were collected and re-dissolved in methylene chloride, passed through a neutral alumina column using methylene chloride as the eluent to remove copper catalysts. The combined eluents were concentrated and precipitated into a mixture of diethyl ether/hexane (1 : 1 v/v). This purification cycle was repeated for three times. The obtained product was dried overnight in a vacuum oven for 24 h ($M_{n,GPC}$ = 4200, M_w/M_n = 1.09; $M_{n,MALDI\text{-}TOF}$ = 2350 Da, PDI = 1.04). It was denoted alkyne-PNIPAM$_{20}$. Following similar procedures, alkyne-PNIPAM precursors with a DP of 10 and 40 were also prepared by adjusting monomer/initiator ratios.

Synthesis of 7-Arm and 21-Arm Star PNIPAM by Click Coupling Reactions

Typical procedures employed for the preparation of 7-arm and 21-arm PNIPAM star polymers were as follows. A mixture of alkyne-PNIPAM$_{20}$ precursor (2.4 g, 1.0 mmol), β-CD-(N$_3$)$_7$ (39 mg, 0.21 mmol azide groups) or β-CD-(N$_3$)$_{21}$ (32 mg, 0.21 mmol azide groups) and DMF (5 mL) was placed in a flask equipped with a magnetic stir bar. The flask was sealed with a rubber septum, evacuated and back-filled with nitrogen for three times. CuBr (100 mg, 0.7 mmol), copper powder (20 mg), and bpy (312 mg, 2mmol) were then added. After stirring under N_2 atmosphere at 60 °C for 48 h, azido-functionalized Merrifield resin was added. The mixture was further stirred at 60 °C for 12 h. After cooling to room temperature and precipitating from DMF into diethyl ether, the product was dissolved in methylene chloride, passed through a neutral alumina column. The combined eluents were evaporated to dryness and then dried to constant weight under vacuum at room temperature. $M_{n,GPC}$ = 33,300, M_w/M_n = 1.04 for β-CD-(PNIPAM$_{20}$)$_7$; $M_{n,GPC}$ = 56,400, M_w/M_n = 1.03 for β-CD-(PNIPAM$_{20}$)$_{21}$. 7-Arm and 21-arm PNIPAM star polymers with the DP of PNIPAM arms being 10 and 40 were also prepared according to similar procedures. The GPC results of the obtained star polymers were summarized in Table 2.

Characterization

Nuclear Magnetic Resonance Spectroscopy

All nuclear magnetic resonance spectroscopy (NMR) spectra were recorded on a Bruker AV300 NMR spectrometer (resonance frequency of 300 MHz for ^{1}H and 75 MHz for ^{13}C) operated in the Fourier transform mode. $CDCl_3$ and DMSO-d_6 were used as the solvent.

Fourier Transform Infrared Spectroscopy

Fourier transform infrared (FTIR) spectra were recorded on a Bruker VECTOR-22 IR spectrometer. The spectra were collected at 64 scans with a spectral resolution of 4 cm^{-1}.

Gel Permeation Chromatography

Molecular weights and molecular weight distributions (M_w/M_n) were determined by gel permeation chromatography (GPC) using a series of three linear Styragel columns (HT2, HT4, and HT5) and an oven temperature of 50 °C. Waters 1515 pump and Waters 2414 differential refractive index detector (set at 30 °C) were used. The eluent was DMF at a flow rate of 1.0 mL/min.

Matrix-Assisted Laser Desorption/Ionization Time-of-Flight Mass Spectrometry

The matrix-assisted laser desorption/ionization time-of-flight (MALDI-TOF) MS was recorded in the linear mode on a Bruker BIFLEXe III mass spectrometer using a nitrogen laser (337 nm) and an accelerating potential of 20 kV. 2,5-Dihydroxybenzoic acid (99%, Sigma) was used as the matrix for PNIPAM ($NaBF_4$ was added to improve the ionization). 1,8,9-Anthracenetriol (99%, Fluka) was used as the matrix for β-CD precursors.

Temperature-Dependent Turbidimetry

The optical transmittance of aqueous solutions of PEMA at a wavelength of 500 nm was acquired on a Unico UV/vis 2802PCS spectrophotometer. A thermostatically controlled couvette was employed and the heating rate was 0.2 °C min^{-1}. The critical phase separation temperature (T_c) was determined as the temperature corresponding to ~1% decrease of optical transmittance.

Micro-Differential Scanning Calorimetry

Micro-differential scanning calorimetry (Micro-DSC) measurements were carried on a VP DSC from MicroCal. The volume of the sample cell was 0.509 mL. The reference cell was filled with deionized water. The sample solution with a

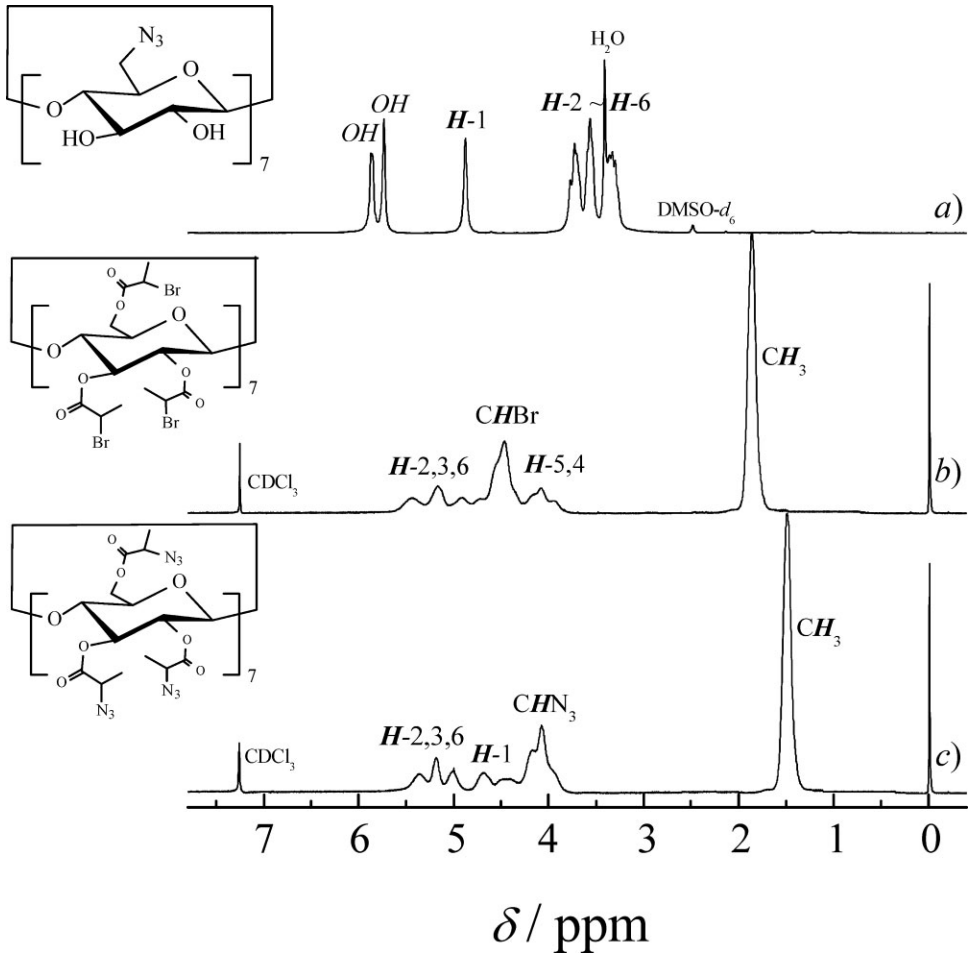

Figure 1. ^{1}H-NMR spectra obtained for (a) β-CD-$(N_3)_7$ in DMSO-d_6, (b) β-CD-$(Br)_{21}$ in $CDCl_3$, and (c) β-CD-$(N_3)_{21}$ in $CDCl_3$.

concentration of 1.0 g/L was degassed at 25 °C for half an hour and equilibrated at 10 °C for 2 h before heating at a rate of 1.0 °C/min.

RESULTS AND DISCUSSION

As shown in Scheme 1, 7-arm and 21-arm star polymers, β-CD-$(PNIPAM)_7$ and β-CD-$(PNIPAM)_{21}$, were synthesized via a combination of click chemistry and ATRP. Firstly core molecules bearing 7 and 21 azide groups, β-CD-$(N_3)_7$ and β-CD-$(N_3)_{21}$, were prepared; alkyne-PNIPAM precursors with varying MW were synthesized via ATRP of *N*-isopropylacrylamide using PCP as an initiator; the subsequent click coupling reaction of alkyne-PNIPAM with β-CD-$(N_3)_7$ and β-CD-$(N_3)_{21}$ led to the facile preparation of 7-arm and 21-arm PNIPAM star polymers, respectively.

Synthesis of Azide-Functionalized β-CD Precursors

To obtain well-defined star polymers via arm-first strategy, it is crucial to choose suitable multifunctional core that can efficiently couple with linear polymer precursors. β-CD bears 7 primary and 14 secondary hydroxyl groups on the peripheral surface, which can be selectively modified via nucleophilic substitution or esterification reaction.

β-CD-$(I)_7$ was prepared via selective replacement of all primary hydroxyl groups of β-CD by iodine atoms. Its subsequent reaction with NaN_3 in DMF led to the formation of β-CD-$(N_3)_7$. ^{1}H-NMR analysis of β-CD-$(N_3)_7$ in DMSO-d_6 [Fig. 1(a)] revealed the complete disappearance of hydroxyl proton (*6*-CH_2OH) signal at 4.5 ppm, which is present in β-CD. ^{13}C-NMR analysis [Fig. 2(a)] also revealed that the signal of *C*-6 shifted from 60.0 ppm in β-CD to 51.5 ppm in β-CD-$(N_3)_7$. The chemical structure of β-CD-$(N_3)_7$ was further

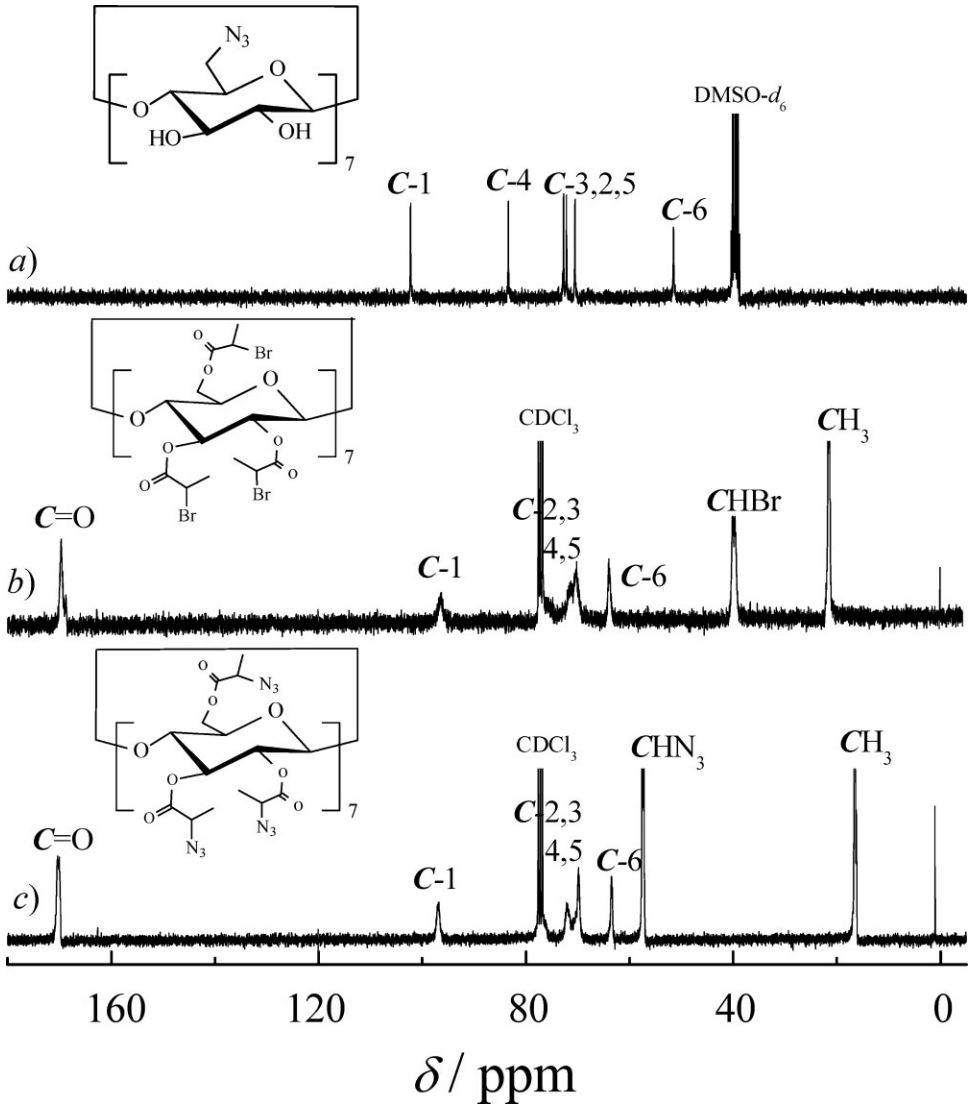

Figure 2. ^{13}C-NMR spectra obtained for (a) β-CD-$(N_3)_7$ in DMSO-d_6, (b) β-CD-$(Br)_{21}$ in $CDCl_3$, and (c) β-CD-$(N_3)_{21}$ in $CDCl_3$.

confirmed by MALDI-TOF MS [Fig. 3(a)]. FTIR spectrum of β-CD-$(N_3)_7$ [Fig. 4(a)] exhibited an absorbance peak at 2105 cm^{-1}, which is characteristic of azide groups.

The complete esterification of β-CD with 2-bromopropionic bromide has been documented previously.[23,59] The procedures reported by Xiao and Li[59] was used for the preparation of β-CD-$(Br)_{21}$ after slight modification. In its ^{1}H-NMR spectrum [Fig. 1(b)], the signals of methine and methyl protons of $BrCHCH_3$ appeared at 4.47 and 1.86 ppm, respectively. ^{13}C-NMR spectrum of β-CD-$(Br)_{21}$ exhibited 2-bromopropionic bromide signals of spectrum [Fig. 2(b)] showed the appearance of signals at 21.5, 39.9, and 169.1 ppm, which can be ascribed to methyl and methine carbons and carbonyl, respectively. MALDI-TOF MS analysis [Fig. 3(a)] further confirmed the structure of β-CD-$(Br)_{21}$ ($[M+H]^+$ = 3947.5, $C_{105}H_{134}O_{56}Br_{21}$ calcd 3948.0). FT-IR spectrum of β-CD-$(Br)_{21}$ revealed the presence of carbonyl absorption peak at 1745 cm^{-1} and the complete disappearance of hydroxyl absorptions at 3400 cm^{-1}. These results indicated that the esterification reaction was 100% complete.

β-CD-$(N_3)_{21}$ was then prepared by reacting β-CD-$(Br)_{21}$ with excess NaN_3 in DMF. ^{1}H and ^{13}C-NMR analysis confirmed the complete nucleophilic substitution [Figs. 1(c) and 2(c)]. The characteristic ^{1}H-NMR signals of methyl protons and

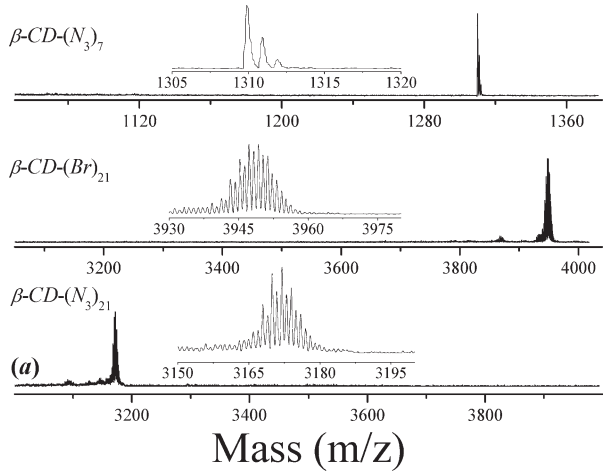

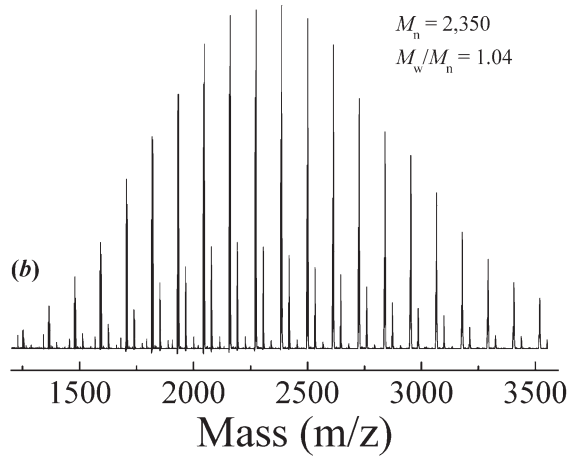

Figure 3. (a) MALDI-TOF mass spectra obtained for β-CD-$(N_3)_7$, β-CD-$(Br)_{21}$, and β-CD-$(N_3)_{21}$ precursors. (b) MALDI-TOF mass spectrum of alkyne-PNIPAM$_{20}$ precursor; the actual degree of polymerization (DP) agrees with the target DP of 20.

methine protons in N_3CHCH_3 appeared at 1.48 and 4.06 ppm for β-CD-$(N_3)_{21}$, which clearly shifted as compared with that of $BrCHCH_3$ (1.86 and 4.47 ppm) in β-CD-$(Br)_{21}$. In addition, ^{13}C-NMR spectrum [Fig. 2(c)] exhibited signals at 16.5 and 57.4 ppm, which can be ascribed to methyl and methine carbons for β-CD-$(N_3)_{21}$. Molecular weights of β-CD-$(N_3)_{21}$ ($[M+H]^+ = 3173.0$, $C_{105}H_{134}O_{56}N_{63}$ calcd 3172.8) determined by MALDI-TOF MS further confirmed its chemical structure [Fig. 3(a)]. Moreover, FTIR spectrum of β-CD-$(N_3)_{21}$ clearly revealed the presence of a new absorbance peak at 2110 cm^{-1}, which is characteristic of azide groups [Fig. 4(a)]. All of these results indicated the successful preparation of β-CD-$(N_3)_{21}$. As expected, β-CD-$(N_3)_{21}$ showed much improved solubility in most organic solvents such as DMF, DMSO, THF, and $CHCl_3$.

GPC traces of β-CD, β-CD-$(N_3)_7$, and β-CD-$(N_3)_{21}$ in DMF was shown in Figure 5, revealing narrow polydispersity in all cases. Table 1 summarized the molecular parameters of β-CD-based precursors.

Preparation of Alkyne-PNIPAM Precursors

The controlled radical polymerization of acrylamido monomers via ATRP has been pioneered by Matyjaszewski and Tsarevsky,[60] Brittain and coworkers,[61] and Masci et al.[62] Recently, Stöver and

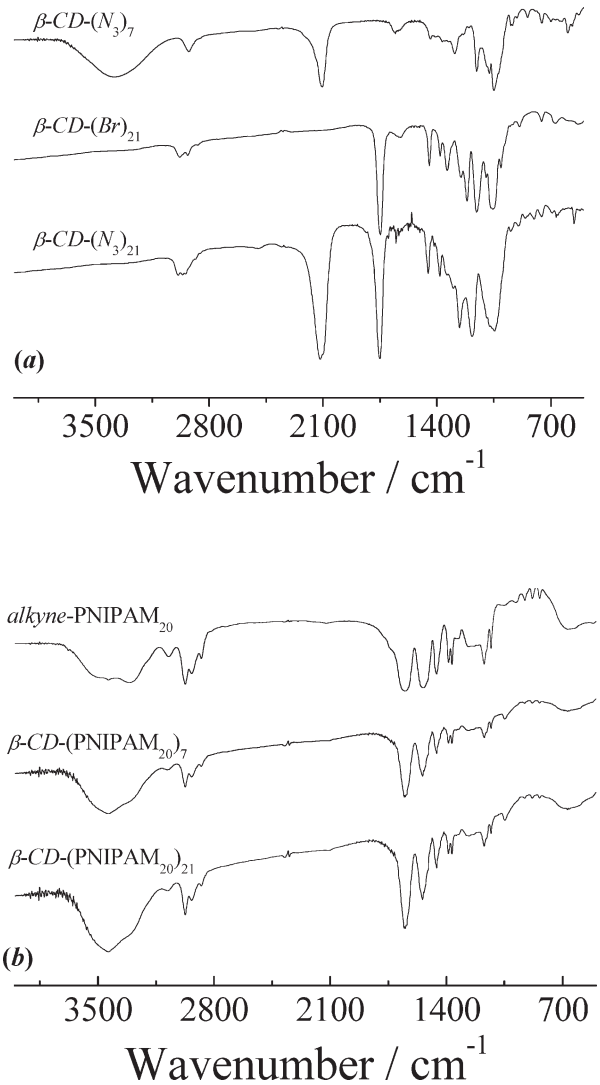

Figure 4. (a) FT-IR spectra obtained for β-CD-$(N_3)_7$, β-CD-$(Br)_7$, and β-CD-$(N_3)_{21}$. (b) FT-IR spectra obtained for alkyne-PNIPAM$_{20}$, β-CD-(PNIPAM$_{20}$)$_7$, and β-CD-(PNIPAM$_{20}$)$_{21}$.

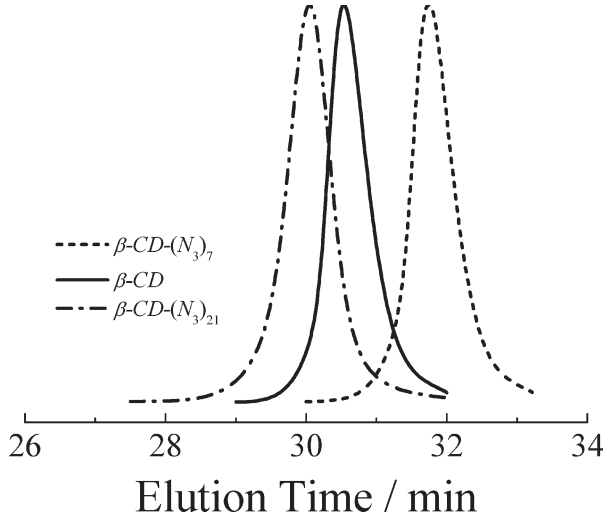

Figure 5. DMF GPC traces obtained for β-CD, β-CD-$(N_3)_7$, and β-CD-$(N_3)_{21}$.

coworkers[63,64] successfully polymerized NIPAM via ATRP in 2-propanol by using methyl 2-chloropropionate as initiator and CuCl/Me_6TREN as catalysts, PNIPAM polymers with controlled MW and narrow polydispersity were obtained.

Lecommandoux and coworkers[65] recently successfully prepared alkynyl terminally functionalized poly(2-(dimethyl-amino)ethyl methacrylate) by ATRP using propargyl 2-bromoisobutyrate as the initiator. In the current study, alkyne-PNIPAM was prepared in 2-propanol by using PCP/CuCl/Me_6TREN system. The MALDI-TOF MS of alkyne-PNIPAM prepared with a target DP of 20 was shown in Figure 3(b). The spectrum shows an envelope of peaks centered at ~2400 Da, extending from 1200 to 3600 Da, giving an $M_{n,MALDI}$ of 2350 Da and M_w/M_n of 1.04. The DP was then calculated to be 20 and the sample was denoted as alkyne-$PNIPAM_{20}$. It should be noted that DP calculated from MALDI-TOF spectrum is quite comparable with that from ^{1}H-NMR.

Using similar procedures, two additional alkyne-PNIPAM samples with different DPs were also prepared. DMF GPC trace of alkyne-PNIPAM with target DP of 10, 20, and 40 were shown in Figure 6(a). All of them revealed relatively sharp and symmetric peaks. No tailing or shoulder at the lower or higher MW side can be discerned, indicating the absence of premature chain termination. This was in good agreement with the results reported by Stöver and coworkers[63,64] The molecular parameters of three alkyne-PNIPAM precursors were summarized in Table 2.

Synthesis of 7-Arm and 21-Arm PNIPAM Star Polymers

Recently, Schubert and coworkers[31] reported the synthesis of 7-arm PCL star polymer via click reaction of alkynyl terminally functionalized linear PCL precursor with β-CD-$(N_3)_7$. Using a similar principle, thermoresponsive water-soluble 7-arm and 21-arm PNIPAM star polymers were prepared via click reactions of alkyne-PNIPAM with β-CD-$(N_3)_7$ and β-CD-$(N_3)_{21}$, respectively, (Scheme 1). To obtain well-defined PNIPAM star polymers with predetermined number of arms, excess alkyne-PNIPAM was used to ensure complete consumption of azido residues in β-CD-$(N_3)_7$ and β-CD-$(N_3)_{21}$. During the preparation of β-CD-$(PNIPAM)_7$ and β-CD-$(PNIPAM)_{21}$ star polymers, [alkyne]/[azide] molar ratio was ~5 : 1 and click reactions were carried out in DMF at 60 °C for 48 h in the presence of CuBr/bpy. Excess alkyne-PNIPAM precursor was facilely removed via click coupling to azido-functionalized Merrifield resin and subsequent suction filtration. Actually, in the preparation of star polymers with short PNIPAM arms (DP = 10), excess alkyne-PNIPAM precursor can be cleanly removed by simple precipitation

Table 1. Structural Characterization of β-CD-Based Precursors and Alkynyl Terminally Functionalized Poly(*N*-isopropylacrylamide) (Alkyne-PNIPAM)

Sample code	$M_{n,GPC}$[a]	M_w/M_n[a]	$M_{n,MALDI}$[b]	M_w/M_n[b]	$M_{n,NMR}$[c]
β-CD-$(N_3)_7$	2,100	1.02	1,310.1	–	–
β-CD-$(Br)_{21}$	4,000	1.02	3,947.5	–	–
β-CD-$(N_3)_{21}$	3,200	1.03	3,172.8	–	–
Alkyne-$PNIPAM_{20}$	4,200	1.09	2,350	1.04	2,400

[a] Number-average molecular weight, M_n, and molecular weight distribution, M_w/M_n, determined by GPC using DMF as eluent.
[b] Measured by MALDI-TOF mass spectrometry.
[c] Determined by ^{1}H NMR in $CDCl_3$.

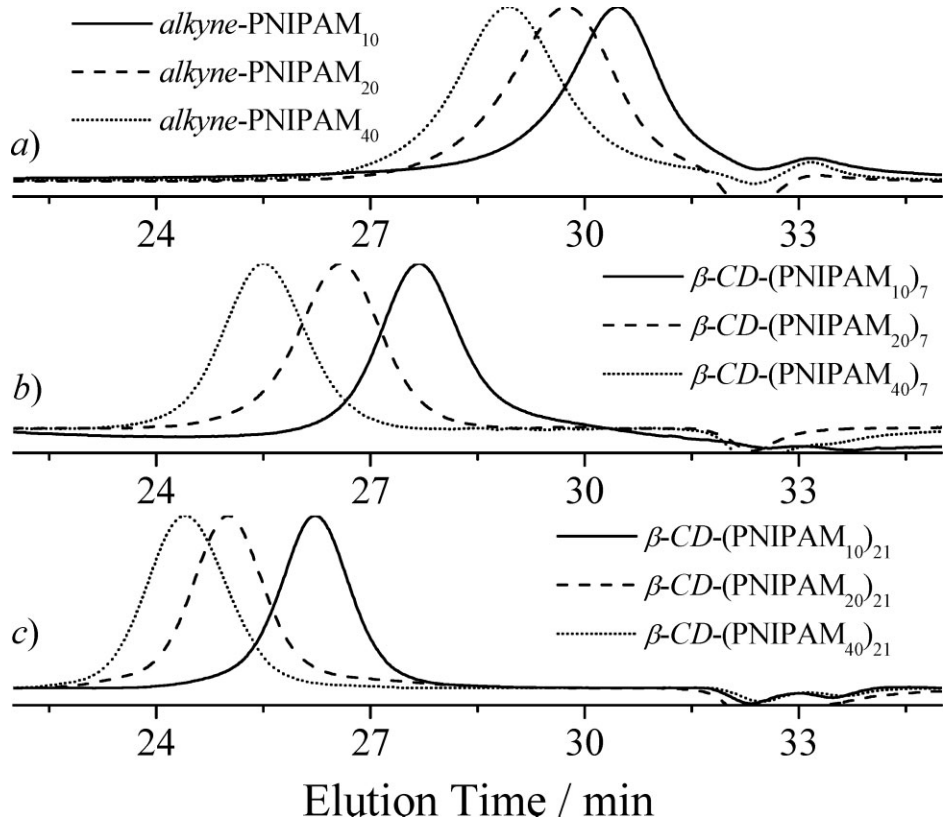

Figure 6. DMF GPC traces obtained for alkyne-PNIPAM, 7-arm and 21-arm PNIPAM star polymers with varying DP for PNIPAM arms.

into diethyl ether because low MW PNIPAM is soluble. In the report by Schubert and coworkers,[31] excess linear PCL precursor was removed by preparative GPC.

GPC traces obtained for 7-arm and 21-arm PNIPAM star polymers with varying arm chain lengths were shown in Figures 6(b and c). All of them were monomodal and relatively symmetric, revealing quite narrow polydispersity. Most importantly, GPC elution peaks of star polymers clearly shifted to higher MW side compared to those of linear PNIPAM precursors and azido-functionalized CD (Figs. 5 and 6). The absence of any tailing at elution times corresponding to that of alkyne-PNIPAM also suggested the complete removal of excess precursors. These results confirmed that the coupling reaction between alkyne-PNIPAM and azido-functionalized β-CD was

Table 2. GPC Characterization Results of *Alkyne*-PNIPAM Precursors, 7-Arm and 21-Arm PNIPAM Star Polymers and Their Critical Phase Separation Temperatures (T_c) in Aqueous Solution

DP of PNIPAM Arms	Alkyne-PNIPAM			β-CD-(PNIPAM)$_7$			β-CD-(PNIPAM)$_{21}$		
	$M_{n,GPC}$[a]	M_w/M_n[a]	T_c (°C)[b]	$M_{n,GPC}$[a]	M_w/M_n[a]	T_c (°C)[b]	$M_{n,GPC}$[a]	M_w/M_n[a]	T_c (°C)[b]
10	3,300	1.09	41	22,700	1.04	33	37,300	1.03	30
20	4,200	1.09	39	33,300	1.04	34	56,400	1.03	31
40	6,900	1.09	38	47,100	1.03	36	67,300	1.04	35

[a] Number–average molecular weight, M_n, and molecular weight distribution, M_w/M_n, determined by GPC using DMF as eluent.

[b] The critical phase separation temperature (T_c) was defined as the temperature corresponding to 1% decrease of optical transmittance (1.0 g/L aqueous solution) at a wavelength of 500 nm, respectively. The estimated error associated with each value was ±1 °C. It should be noted that the T_c value obtained in the current study should be better viewed as the onset temperature of interchain aggregation.

highly efficient. GPC characterization results of a series of six β-CD-(PNIPAM)$_7$ and β-CD-(PNIPAM)$_{21}$ star polymers were summarized in Table 2. Figure 4(b) shows FT-IR spectra of β-CD-(PNIPAM$_{20}$)$_7$ and β-CD-(PNIPAM$_{20}$)$_{21}$. A comparison to those of β-CD-(N$_3$)$_7$ and β-CD-(N$_3$)$_{21}$ [Fig. 4(a)] revealed the complete disappearance of characteristic azide absorbance peak at ~2110 cm^{-1} for 7-arm and 21-arm PNIPAM star polymers. This further confirmed that click reactions were qualitatively complete.

Thermal Phase Transition Behavior of 7-Arm and 21-Arm PNIPAM Star Polymers

For β-CD-(PNIPAM)$_7$, the average distance between two neighboring grafted chains on the narrow side of the truncated cone can be estimated to be 0.62 nm; whereas for β-CD-(PNIPAM)$_{21}$, the average distances on the narrow and wide sides of truncated cone were estimated to be 0.62 and 0.34 nm, respectively.[12,66] As these characteristic distances are much smaller than the dimension of grafted PNIPAM chain with DP in the range of 10-40, 7-arm, and 21-arm PNIPAM star polymers can then be considered as densely grafted polymer brushes at the surface of β-CD cores.

Chain Architecture Effects on the Phase Transition Behavior

Table 2 lists the critical phase separation temperatures (T_c) of three linear alkyne-PNIPAM precursors with DP being 10, 20, and 40, respectively. It should be noted that the definition of T_c in the current study (temperature corresponding to 1% decrease of transmittance) can be better considered as the onset temperature of aggregation (Fig. 7). The classical definition of LCST should be the temperature minimum on the coexistance curve. We found that T_c decreased from 41 to 38 °C when the DP of alkyne-PNIPAM increased from 10 to 40. Although the MW dependence of T_c is in general agreement with that reported for methoxypropionate-terminated PNIPAM by Stöver and coworkers,[63,64] the magnitude of the variation of T_c with MW for alkyne-PNIPAM is much smaller. This discrepancy should be ascribed to differences in hydrophobicity of terminal groups.

Figure 7(a) shows the temperature-dependent optical transmittance for alkyne-PNIPAM$_{20}$, β-CD-(PNIPAM$_{20}$)$_7$, and β-CD-(PNIPAM$_{20}$)$_{21}$ star polymers in aqueous solution at a concentration

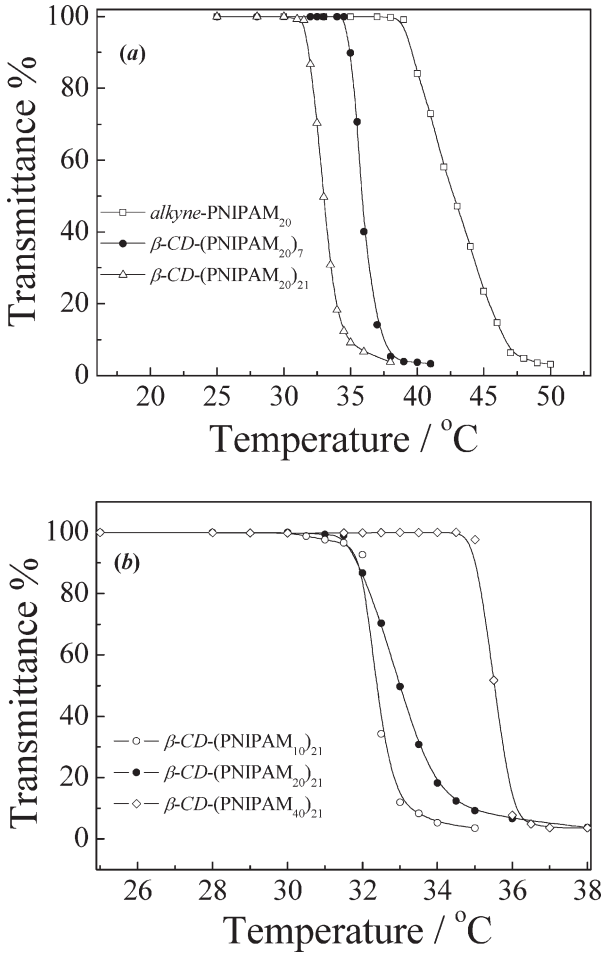

Figure 7. (a) Temperature dependence of optical transmittance at 500 nm obtained for 1.0 g/L aqueous solutions of alkyne-PNIPAM$_{20}$, β-CD-(PNIPAM$_{20}$)$_7$, and β-CD-(PNIPAM$_{20}$)$_{21}$. (b) Temperature dependence of optical transmittance at 500 nm obtained for 1.0 g/L aqueous solutions of β-CD-(PNIPAM$_{10}$)$_{21}$, β-CD-(PNIPAM$_{20}$)$_{21}$, and β-CD-(PNIPAM$_{40}$)$_{21}$ star polymers.

of 1.0 g/L, revealing T_c values of 39, 34, and 31 °C, respectively. The considerably lower T_c values for 7-arm and 21-arm star polymers compared to that of linear precursor should be ascribed to the dense packing of PNIPAM chains at the surface of CD cores for star polymers. The local high chain density for star polymers led to their collapse and aggregation at lower temperatures, possibly due to the formation of *n*-clusters.[53,54] From Table 2, we can conclude that 7-arm and 21-arm star polymers with varying MW typically possessed lower T_c than linear precursors. Surely, the molecular weights of PNIPAM star polymers are much larger than the linear precursor. Although this can explain the decrease of T_c in star

polymers,[63,64] subsequent micro-DSC data will elucidate that the difference in spatial arrangement of PNIPAM chains is the dominating factor for the decrease of T_c in star polymers.

We then measured the partial heat capacity (C_p) of alkyne-PNIPAM$_{20}$, β-CD-(PNIPAM$_{20}$)$_7$, and β-CD-(PNIPAM$_{20}$)$_{21}$ in aqueous solution by micro-DSC. Figure 8(a) shows the temperature dependence of partial heat capacity (C_p) of aqueous solutions at a concentration of 1.0 g/L. It has been established that microcalorimetry can detect the disruption of hydrogen bonds between amide groups and water molecule during the collapse and aggregation of PNIPAM chains. For linear PNIPAM with high MW ($>10^4$ Da), enthalpy change (ΔH) associated with the thermal phase transition has been determined to be in the range of 5.5–7.5 kJ per mole of NIPAM repeating units.[49,63] For alkyne-PNIPAM$_{20}$, micro-DSC curve revealed one broad endothermic peak with ΔH of 3.9 kJ/mol, which is quite comparable to that reported by Stöver et al.[63] for PNIPAM with comparable MW. It should be noted that the broad temperature range measured by microcalorimetry is typical of low MW PNIPAM chains.

On the other hand, micro-DSC analysis of β-CD-(PNIPAM$_{20}$)$_7$ and β-CD-(PNIPAM$_{20}$)$_{21}$ star polymers revealed relatively sharp endothermic peaks, giving ΔH of 2.9 and 3.0 kJ per mole of NIPAM repeating units, respectively, [Fig. 8(a)]. The molecular weights of β-CD-(PNIPAM$_{20}$)$_7$ and β-CD-(PNIPAM$_{20}$)$_{21}$ were calculated to be $\sim 1.7 \times 10^4$ and 4.9×10^4, respectively. The considerably lower ΔH for 7-arm and 21-arm star polymers compared to alkyne-PNIPAM$_{20}$ and linear PNIPAM with comparable MW (5.5–7.5 kJ/mol) strongly suggested chain architecture effects on the strength of hydrogen bonds between amide moiety and water molecules. Compared to those in linear chains, water molecules in star polymers are much less structured and more mobile due to the high local chain density, that is, the steric constraints existing for star polymers will arrest the formation of hydration structures to a large extent considering the orientations of hydrogen bonds. Therefore, hydrogen bonds formed around linear PNIPAM chains are stronger and more stable.

On the other hand, during thermal phase transition, the loss of conformational entropy for star polymers will be smaller than that for linear PNIPAM. The phase transition was driven by the large positive change of translational entropy of water molecules released due to disruption of hydrogen bonds. The overall entropy change for star polymer chains is more positive so that it requires a lower phase transition temperature to render the change of free energy to be negative. It is worthy of noting that T_c of β-CD-(PNIPAM$_{20}$)$_7$ (34 °C) was larger than that of β-CD-(PNIPAM$_{20}$)$_{21}$ (31 °C), this might be ascribed to that the latter possessed a much larger grafting chain density.

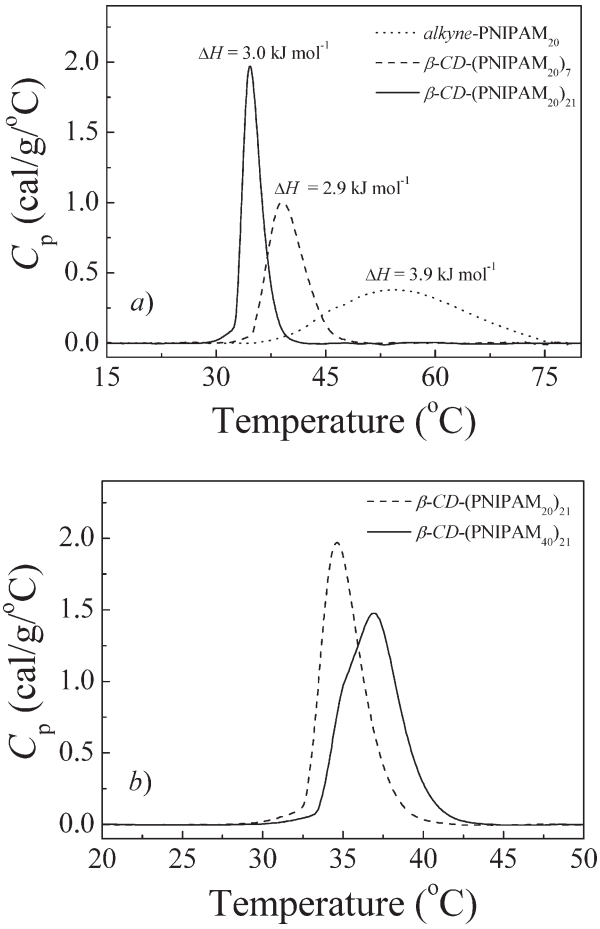

Figure 8. (a) Temperature dependence of specific heat capacity (C_p) obtained for 1.0 g/L aqueous solutions of alkyne-PNIPAM$_{20}$, β-CD-(PNIPAM$_{20}$)$_7$, β-CD-(PNIPAM$_{20}$)$_{21}$. (b) Temperature dependence of specific heat capacity (C_p) obtained for 1.0 g/L aqueous solutions of β-CD-(PNIPAM$_{20}$)$_{21}$ and β-CD-(PNIPAM$_{40}$)$_{21}$ star polymers.

MW Dependence of Phase Transition Behavior of Star Polymers

Previous reports of the phase transition behavior of PNIPAM brushes tethered at the surface of curved surfaces (e.g., latex particles,[46–48] gold

nanoparticles,[49,50] microgels,[51] and hyperbranched polymers[8,57,67]) suggested double phase transition behavior. This is due to that the inner part of PNIPAM segments close to the core is more densely packed than the outer part. Then the former typically exhibits collapse at temperatures considerably lower than the LCST of free PNIPAM chains in solution due to *n*-cluster formation. For PNIPAM chains adsorbed at the surface of latex particles, Napper and coworkers[46–48] observed that the *n*-cluster contribution increased significantly with decreasing MW of PNIPAM chains. On the contrary, Whittaker and coworkers[55] reported that for 4-arm PNIPAM star polymers with varying MW, *n*-cluster contribution increased with increasing MW for star polymers. The apparent discrepancy between these two examples might be ascribed to the fact that grafting densities at the core surface and MW range of PNIPAM chains differ considerably. Thus, further investigations are necessary to understand the chain length effects on the phase transition behavior of PNIPAM brushes at the surface of a spherical core.

Figure 7(b) shows typical temperature-dependent optical transmittance for β-CD-(PNIPAM)$_{21}$ star polymers with varying MW. The critical phase separation temperatures, T_c, for all six star polymers with varying grafting number and arm lengths were summarized in Table 2. Unexpectedly, we found that T_c values increased with increasing DP of PNIPAM arms for β-CD-(PNIPAM)$_7$ and β-CD-(PNIPAM)$_{21}$ star polymers, which was contrary to that observed for linear PNIPAM chains.[63,64] It should be noted that Whittaker et al. observed similar phenomenon, and they ascribed it to the presence of hydrophobic star core and surface benzyl groups.

For β-CD-(PNIPAM)$_{21}$, the fully functionalized CD core is indeed hydrophobic. This may interfere with the contribution of *n*-clustering induced early collapse of PNIPAM inner brush. It is well-known that the phase transition temperature of PNIPAM will considerably decrease in the presence of hydrophobic terminal groups. On the other hand, for β-CD-(PNIPAM)$_7$, the CD core is hydrophilic due to the presence of 14 hydroxyl groups and 7 triazole moieties. However, for both β-CD-(PNIPAM)$_7$ and β-CD-(PNIPAM)$_{21}$ star polymers, T_c increased with increasing DP of PNIPAM arm in the range of 10–40 (Table 2). Thus, the interference of core hydrophobicity on the phase transition can be safely excluded, especially in the case of β-CD-(PNIPAM)$_7$.

Figure 8(b) compares micro-DSC results of β-CD-(PNIPAM$_{20}$)$_{21}$ and β-CD-(PNIPAM$_{40}$)$_{21}$ star polymers. Interestingly, we found that DSC curve of β-CD-(PNIPAM$_{20}$)$_{21}$ is relatively symmetric, whereas that of β-CD-(PNIPAM$_{40}$)$_{21}$ clearly exhibits a slight shoulder peak at the lower temperature side. This strongly suggests that the phase transition of β-CD-(PNIPAM$_{40}$)$_{21}$ might possess two partially overlapping transitions. Here we propose a tentative explanation by invoking *n*-cluster concepts. As the local chain density in PNIPAM brush grafted at a spherical core possessed an exponentially decreasing gradient from the inner to outer layer, it can in principle be expected that PNIPAM star polymers with varying MW might behave considerably different. For low MW star polymers, *n*-cluster induced collapse will lead to prominent decrease of critical phase transition temperature as the chain density remains to be high even at the outer layer. For higher MW star polymers, the clustering-induced collapse of the inner layer can be stabilized by the swollen outer layer. The collapse and aggregation of the outer layer will typically occur at elevated temperatures due to the lower local chain density. The above argument can also reasonably explain the increase of T_c with the increase of MW for 7-arm star polymers. Thus, the contribution of clustering-induced collapse to thermal phase transition was prominent for low molecular weight star polymers, and it will decrease with increasing arm lengths.

CONCLUSIONS

Well-defined 7-arm and 21-arm poly(*N*-isopropylacrylamide) (PNIPAM) star polymers possessing β-CD cores have been synthesized via click reactions of alkynyl-terminated linear PNIPAM of varying DPs with β-CD-(N$_3$)$_7$ and β-CD-(N$_3$)$_{21}$, respectively. The thermal phase transition behavior of β-CD-(PNIPAM)$_7$ and β-CD-(PNIPAM)$_{21}$ star polymers with varying molecular weights has been examined by temperature-dependent turbidity and micro-differential scanning calorimetry (micro-DSC). Both the anchoring of PNIPAM chain terminal to β-CD cores and high local chain density for star polymers contributed to their much lower critical phase separation temperatures (T_c) and enthalpy changes during phase transition as compared to those of linear precursors. Unexpectedly, we observed that T_c of β-CD-(PNIPAM)$_{21}$ and β-CD-(PNIPAM)$_7$ considerably

increased with increasing DP of PNIPAM arms, which was contrary to that of linear PNIPAM. This strongly suggested *n*-cluster formation for PNIPAM segments at the immediate surface of β-CD core due to its high chain grafting density. The contribution of clustering-induced collapse to thermal phase separation was prominent for low MW star polymers. On the other hand, for β-CD-$(PNIPAM)_{21}$ star polymer with high MW, the collapse of inner chain segments can be stabilized by the outer layer. The collapse and aggregation of the outer layer occurred at elevated temperatures due to its much lower local chain density. Although the above argument can qualitatively explain the MW dependence of T_c for star polymers, more complementary evidences need to be collected in the future.

The financial supports of National Natural Scientific Foundation of China (NNSFC) Projects (20534020, 20674079, 50425310), Specialized Research Fund for the Doctoral Program of Higher Education (SRFDP), and the Program for Changjiang Scholars and Innovative Research Team in University (PCSIRT) are gratefully acknowledged.

REFERENCES AND NOTES

1. Hadjichristidis, N.; Pitsikalis, M.; Iatrou, H. Adv Polym Sci 2005, 189, 1–124.
2. Hadjichristidis, N.; Pitsikalis, M.; Pispas, S.; Iatrou, H. Chem Rev 2001, 101, 3747–3792.
3. Inoue, K. Prog Polym Sci 2000, 25, 453–571.
4. Taton, D.; Gnanou, Y.; Matmour, R.; Angot, S.; Hou, S.; Francis, R.; Lepoittevin, B.; Moinard, D.; Babin, J. Polym Int 2006, 55, 1138–1145.
5. Hou, S. J.; Chaikof, E. L.; Taton, D.; Gnanou, Y. Macromolecules 2003, 36, 3874–3881.
6. Chen, Y.; Shen, Z.; Barriau, E.; Kautz, H.; Frey, H. Biomacromolecules 2006, 7, 919–926.
7. Luo, S. Z.; Xu, J.; Zhu, Z. Y.; Wu, C.; Liu, S. Y. J Phys Chem B 2006, 110, 9132–9139.
8. Xu, J.; Luo, S. Z.; Shi, W. F.; Liu, S. Y. Langmuir 2006, 22, 989–997.
9. Miura, Y.; Dote, H. J Polym Sci Part A: Polym Chem 2005, 43, 3689–3700.
10. Yuan, W. Z.; Yuan, J. Y.; Zhou, M.; Pan, C. Y. J Polym Sci Part A: Polym Chem 2008, 46, 2788–2798.
11. Yuan, W. Z.; Yuan, J. Y.; Zhou, M.; Sui, X. F. J Polym Sci, Part A: Polym Chem 2006, 44, 6575–6586.
12. Ritter, H.; Tabatabai, M. Prog Polym Sci 2002, 27, 1713–1720.
13. Hawker, C. J.; Bosman, A. W.; Harth, E. Chem Rev 2001, 101, 3661–3688.
14. Wang, J. S.; Matyjaszewski, K. Macromolecules 1995, 28, 7901–7910.
15. Matyjaszewski, K.; Xia, J. H. Chem Rev 2001, 101, 2921–2990.
16. Plamper, F. A.; Schmalz, A.; Penott-Chang, E.; Drechsler, M.; Jusufi, A.; Ballauff, M.; Muller, A. H. E. Macromolecules 2007, 40, 5689–5697.
17. Chiefari, J.; Chong, Y. K.; Ercole, F.; Krstina, J.; Jeffery, J.; Le, T. P. T.; Mayadunne, R. T. A.; Meijs, G. F.; Moad, C. L.; Moad, G.; Rizzardo, E.; Thang, S. H. Macromolecules 1998, 31, 5559–5562.
18. Chong, Y. K.; Le, T. P. T.; Moad, G.; Rizzardo, E.; Thang, S. H. Macromolecules 1999, 32, 2071–2074.
19. Kakuchi, T.; Narumi, A.; Matsuda, T.; Miura, Y.; Sugimoto, N.; Satoh, T.; Kaga, H. Macromolecules 2003, 36, 3914–3920.
20. Karaky, K.; Reynaud, S.; Billon, L.; Francois, J.; Chreim, Y. J Polym Sci Part A: Polym Chem 2005, 43, 5186–5194.
21. Li, J. S.; Xiao, H. N.; Kim, Y. S.; Lowe, T. L. J Polym Sci Part A: Polym Chem 2005, 43, 6345–6354.
22. Miura, Y.; Narumi, A.; Matsuya, S.; Satoh, T.; Duan, Q.; Kaga, H.; Kakuchi, T. J Polym Sci Part A: Polym Chem 2005, 43, 4271–4279.
23. Ohno, K.; Wong, B.; Haddleton, D. M. J Polym Sci Part A: Polym Chem 2001, 39, 2206–2214.
24. Plamper, F. A.; Becker, H.; Lanzendorfer, M.; Patel, M.; Wittemann, A.; Ballauf, M.; Muller, A. H. E. Macromol Chem Phys 2005, 206, 1813–1825.
25. Stenzel, M. H.; Davis, T. P. J Polym Sci Part A: Polym Chem 2002, 40, 4498–4512.
26. Stenzel, M. H.; Davis, T. P.; Fane, A. G. J Mater Chem 2003, 13, 2090–2097.
27. Stenzel-Rosenbaum, M. H.; Davis, T. P.; Chen, V. K.; Fane, A. G. Macromolecules 2001, 34, 5433–5438.
28. Finn, M. G.; Kolb, H. C.; Fokin, V. V.; Sharpless, K. B. Prog Chem 2008, 20, 1–4.
29. Kolb, H. C.; Finn, M. G.; Sharpless, K. B. Angew Chem Int Ed 2001, 40, 2004–2021.
30. Gao, H. F.; Matyjaszewski, K. Macromolecules 2006, 39, 4960–4965.
31. Hoogenboom, R.; Moore, B. C.; Schubert, U. S. Chem Commun 2006, 4010–4012.
32. Diaz, D. D.; Punna, S.; Holzer, P.; Mcpherson, A. K.; Sharpless, K. B.; Fokin, V. V.; Finn, M. G. J Polym Sci Part A: Polym Chem 2004, 42, 4392–4403.
33. Li, C. M.; Finn, M. G. J Polym Sci Part A: Polym Chem 2006, 44, 5513–5518.
34. Liu, Y.; Diaz, D. D.; Accurso, A. A.; Sharpless, K. B.; Fokin, V. V.; Finn, M. G. J Polym Sci Part A: Polym Chem 2007, 45, 5182–5189.

35. Altintas, O.; Demirel, A. L.; Hizal, G.; Tunca, U. J Polym Sci Part A: Polym Chem 2008, 46, 5916–5928.
36. Urbani, C. N.; Lonsdale, D. E.; Bell, C. A.; Whittaker, M. R.; Monteiro, M. J. J Polym Sci Part A: Polym Chem 2008, 46, 1533–1547.
37. Jiang, X. Z.; Zhang, J. Y.; Zhou, Y. M.; Xu, J.; Liu, S. Y. J Polym Sci Part A: Polym Chem 2008, 46, 860–871.
38. Takizawa, K.; Nulwala, H.; Thibault, R. J.; Lowenhielm, P.; Yoshinaga, K.; Wooley, K. L.; Hawker, C. J. J Polym Sci Part A: Polym Chem 2008, 46, 2897–2912.
39. Wang, G. W.; Luo, X. L.; Liu, C.; Huang, J. L. J Polym Sci Part A: Polym Chem 2008, 46, 2154–2166.
40. Shi, G. Y.; Tang, X. Z.; Pan, C. Y. J Polym Sci Part A: Polym Chem 2008, 46, 2390–2401.
41. Yang, L. P.; Zhou, H. X.; Shi, G. Y.; Wang, Y.; Pan, C. Y. J Polym Sci Part A: Polym Chem 2008, 46, 6641–6653.
42. Billiet, L.; Fournier, D.; Prez, F. D. J Polym Sci Part A: Polym Chem 2008, 46, 6552–6564.
43. Dag, A.; Durmaz, H.; Demir, E.; Hizal, G.; Tunca, U. J Polym Sci Part A: Polym Chem 2008, 46, 6969–6977.
44. Rzaev, Z. M. O.; Dincer, S.; Piskin, E. Prog Polym Sci 2007, 32, 534–595.
45. Furyk, S.; Zhang, Y. J.; Ortiz-Acosta, D.; Cremer, P. S.; Bergbreiter, D. E. J Polym Sci Part A: Polym Chem 2006, 44, 1492–1501.
46. Zhu, P. W.; Napper, D. H. Colloids Surf A 1996, 113, 145–153.
47. Turner, K.; Zhu, P. W.; Napper, D. H. Colloid Polym Sci 1996, 274, 622–627.
48. Zhu, P. W.; Napper, D. H. J Colloid Interface Sci 1994, 164, 489–494.
49. Shan, J.; Chen, J.; Nuopponen, M.; Tenhu, H. Langmuir 2004, 20, 4671–4676.
50. Shan, J.; Tenhu, H. Chem Commun 2007, 4580–4598.
51. Hu, T. J.; Wu, C. Phys Rev Lett 1999, 83, 4105–4107.
52. Halperin, A.; Tirrell, M.; Lodge, T. P. Adv Polym Sci 1992, 100, 31–71.
53. Wagner, M.; Brochardwyart, F.; Hervet, H.; Degennes, P. G. Colloid Polym Sci 1993, 271, 621–628.
54. Degennes, P. G. C R l'Academie Sci, Ser II Univers 1991, 313, 1117–1122.
55. Plummer, R.; Hill, D. J. T.; Whittaker, A. K. Macromolecules 2006, 39, 8379–8388.
56. Zhang, Z. X.; Liu, X.; Xu, F. J.; Loh, X. J.; Kang, E. T.; Neoh, K. G.; Li, J. Macromolecules 2008, 41, 5967–5970.
57. Xu, J.; Ye, J.; Liu, S. Y. Macromolecules 2007, 40, 9103–9110.
58. Ashton, P. R.; Koniger, R.; Stoddart, J. F.; Alker, D.; Harding, V. D. J Org Chem 1996, 61, 903–908.
59. Li, J. S.; Xiao, H. N. Tetrahedron Lett 2005, 46, 2227–2229.
60. Tsarevsky, N. V.; Matyjaszewski, K. Chem Rev 2007, 107, 2270–2299.
61. Rademacher, J. T.; Baum, R.; Pallack, M. E.; Brittain, W. J.; Simonsick, W. J. Macromolecules 2000, 33, 284–288.
62. Masci, G.; Giacomelli, L.; Crescenzi, V. Macromol Rapid Commun 2004, 25, 559–564.
63. Xia, Y.; Burke, N. A. D.; Stover, H. D. H. Macromolecules 2006, 39, 2275–2283.
64. Xia, Y.; Yin, X.; Burke, N.; Stover, H. Macromolecules 2005, 38, 5937–5943.
65. Agut, W.; Taton, D.; Lecommandoux, S. Macromolecules 2007, 40, 5653–5661.
66. Szejtli, J.Cyclodextrin Technology; Kluwer: Dordrecht, 1988; p 12.
67. Carter, S.; Hunt, B.; Rimmer, S. Macromolecules 2005, 38, 4595–4603.